

# The Use of $^{19}\text{F}$ NMR to Interpret the Structural Properties of Perfluorocarboxylate Acids: A Possible Correlation with Their Environmental Disposition

David A. Ellis,<sup>†</sup> Kerri A. Denkenberger,<sup>‡</sup> Timothy E. Burrow,<sup>†</sup> and Scott A. Mabury<sup>\*,†</sup>

Department of Chemistry, University of Toronto, 80 St. George Street, Toronto, ON, Canada M5S 3H6, and Department of Chemistry, 152 Davey Laboratory, The Pennsylvania State University, University Park, Pennsylvania 16802

Received: February 11, 2004; In Final Form: August 30, 2004

The use of perfluorinated anionic carboxylic acids (PFCAs) as surfactants is common and widespread. Investigations of PFCAs have shown that their physical properties and toxicological aspects are dependent upon the carbon chain length. The magnitude of these properties is not a linear function of chain length and as yet no explanation of these unique observations has been made. Their environmental dissemination is expected to be nonproportional to the PFCAs chain length. An understanding of the fundamental underlying reason for this novel physical property, chain length trend, would aid further investigators' interpretation of their environmental and toxicological observations. In this study we have utilized  $^{19}\text{F}$  NMR techniques, such as, chemical shift, spin–lattice ( $T_1$ ), and spin–spin ( $T_2$ ) relaxation phenomena, coupling constants, and variable-temperature NMR to furnish a qualitative explanation of why increasing the carbon chain length causes unexpected intrinsic property changes within this group of chemicals. Results indicate that polyfluorinated chains adopt helical twist geometry unlike their hydrocarbon counterparts which exhibit a zigzag geometry. Variable-temperature  $^{19}\text{F}$  NMR showed that chain rigidity within these molecules is also a function of the fluorocarbon chain length. There is a distinct change in geometry and rigidity of the acid chain between 8 and 10 carbon lengths. These unique geometric changes in this class of compound must be considered when assessing their dissemination in the environment, for example, in the case of environmental modeling.

## 1. Introduction

The incorporation of fluorine within anthropogenically produced materials is vast,<sup>1</sup> of which a subclass is anionic fluorinated surfactants. They are used as adhesives, antifogging and antistatic agents, firefighting foams and powders, emulsifiers, and in the etching and surface treatment of glasses, to name but a few.<sup>2</sup> These surfactants can be further subdivided into four main categories: carboxylates, sulfonates, sulfates, and phosphates; and in the present studies, we have limited our focus to the perfluorocarboxylates (PFCAs) whose conjugate acids have the general structure  $\text{CF}_3(\text{CF}_2)_n\text{COOH}$  ( $n = 2–12$ ).

PFCAs and perfluorosulfonates (PFSs) have been shown to be widely disseminated in the natural environment.<sup>3–10</sup> In fact the US EPA has recently published a notice for, “the publication within the Federal Register on perfluorooctanoic acid (PFOA)”. With this Notice, the EPA is releasing a preliminary risk assessment on PFOA, and is starting a public process to identify and generate additional information to strengthen the risk assessment of this and related chemicals.<sup>11</sup>

It is still unclear how these molecules are transported in the environment; however, it can be assumed that this wide dissemination must be in part due to the unique intrinsic physical properties which fluorine imparts upon the molecule.<sup>11,12</sup> A clear understanding of the underlying effects that fluorination has upon the molecule may in turn lead to a better understanding of their modes of transport and dissemination in the environment.

The introduction of fluorine within the structure often results in physical properties that are not always intuitively predictable.

An example of this is seen in a comparison of the melting and boiling points of fluorinated surfactants; fluorinated surfactants melt at higher temperatures than their hydrocarbon analogues although they have much lower boiling points.<sup>2</sup> This effect is reportedly due to the “stiffness” of the fluorinated chain that is described as being hard and inflexible.<sup>2</sup> Eaton and Smart have shown that the energy of bending and folding of the fluorocarbon chain is significantly greater than that for the corresponding hydrocarbon chain ( $\approx 2.5$  kcal/mol greater activation energy barrier).<sup>14</sup>

Increasing the linear fluorocarbon chain reportedly results in interesting changes to the solid-phase structural geometry of the chain. For example, in the case of semifluorinated 1-bromoalkanes, it has been shown that, as the perfluorocarbon chain length is increased, the molecules' geometry changes from a planar zigzag configuration to a helical structure.<sup>15</sup> The chain conformation is described as being zigzag for chain lengths of 8 carbons and less, a mixture of zigzag and helical for chain lengths of 8–12 carbons, and fully helical for chain lengths greater than 12 carbon atoms. Knochenhauer et al. have shown, using diffraction data and molecular calculations, that perfluorodecanoic acid adopts a helical conformation; however, the molecules return to a linear conformation when packed into a periodic lattice.<sup>16</sup> Erkoç and Erkoç have also shown that the predicted conformation of PFOS is helical; however, replacing the  $\text{H}^+$  for  $\text{Li}^+$  results in the molecule adopting a near-linear conformation.<sup>17</sup> Thus, it would appear that the conformation that the perfluorinated tail takes on depends not only on the length of the carbon chain itself, but also upon the functional group attached to it and upon the molecules immediate environment. It is worth noting that these studies have focused upon the solid-state conformation of perfluorinated chains, while

\* To whom correspondence should be addressed. E-mail: smabury@chem.utoronto.ca. Phone: (416) 978-1780. Fax: (416) 978-3596.

<sup>†</sup> University of Toronto.

<sup>‡</sup> The Pennsylvania State University.

little research has been conducted in the assessment of the solution-phase conformation of these molecules, especially for the short chain species. Given that, environmentally, the PFCAs have been found predominately in the solution phase a further understanding of the conformations adopted by the molecule would be a great asset.

$^{19}\text{F}$  NMR can play an important role in ascertaining the underlying fundamental microscopic molecular properties that give rise to the macroscopic physical properties observed. For example, using  $^{13}\text{C}$ -detected,  $^{19}\text{F}$ -decoupled separated-local-field (SCF) spectroscopy, Dvinskikh and Furó have shown that, in the case of the cesium salt of perfluorooctanoic acid, fluorination of the carbon chain results in a significantly more rigid structure than is the case for the hydrocarbon counterpart.<sup>18</sup>

Although extremely useful in identifying the physical properties of a molecule, spin–spin splitting patterns in the  $^{19}\text{F}$  NMR spectra of perfluorinated acids are often very complex and unresolvable. This is a result of long-range coupling that occurs over at least 4 bonds.<sup>19</sup> Coupling constants have been reported for perfluorobutyric acid, although, due to spectral overlap, only one coupling constant could be fully established, i.e.,  $J_{\text{FF}} = 9.9$  Hz between the terminal  $\text{CF}_3$  and the  $\text{CF}_2$  adjacent to the carboxylate functional group.<sup>20</sup>

The acquisition of  $^{19}\text{F}$  NMR coupling constants for highly fluorinated molecules would be extremely advantageous in determining molecular dynamics, such as molecular geometry (e.g., torsional angles), chain rigidity, and conformation.

As the number of fluorine nuclei and molecular size increase, both the location and assignment of the fluorine resonances become increasingly difficult. Thus, extensive work has been conducted by Weigert and Karel and Bauduin et al. to develop calculation models that predict the chemical shifts for saturated fluorocarbons.<sup>21,22</sup> Ribeiro has employed an  $^{19}\text{F}$  detected HMQC and HMBC experiment to assign  $^{19}\text{F}$  and  $^{13}\text{C}$  chemical shifts for the highly fluorinated alcohol *1H,1H,2H,2H*-tridecafluorooctanol ( $\text{CF}_3(\text{CF}_2)_5\text{CH}_2\text{CH}_2\text{OH}$ ).<sup>23</sup> Fluorinated alcohols of this nature have also been studied by other researchers.<sup>24–26</sup> Interesting structural information concerning the geometry of the molecule and electron density distributions was obtained through analysis of changes in chemical shifts, coupling constants, spin–lattice relaxation times, and nuclear Overhauser enhancement (NOE) effects. These techniques have shown that the fluorocarbon chain is rigid. Measurements of both the  $T_1$  and  $T_2$  relaxation of the fluorine nuclei can often lead to important observations concerning the environment of the molecule and its geometry.

In short, as a molecules' physical properties, and their predication, rely, to a certain extent, upon the physical state and nature of the molecule, understanding the geometry adopted by perfluorinated acids may shed light upon the distribution processes in the environment. For example, knowing if the molecule adopts a hydrophobic rigid helical rod-like tail, or if is flexible, would change the way in which researchers might view various environmental partition coefficients.

Previous investigations of the structural nature of polyfluorinated systems have been limited by the inability for the determination of long-range  $^{19}\text{F}$ – $^{19}\text{F}$  coupling constants. To resolve this issue our novel approach was to employ a 2D  $J$  resolved pulse sequence. Taken in conjunction with other key NMR and physical parameters, such as temperature, it was hypothesized that this would allow for key information to be obtained concerning the geometrical nature and structural properties of a perfluorinated carbon chain. It was proposed that the study be expanded to systematically investigate these

properties as a function of the chain length and to relate any chain length variances to those empirically observed in their environmental and biological behavior.

## 2. Experimental Section

All chemicals were obtained as follows: perfluorotetradecanoic acid, perfluoroundecanoic acid [3M (Minnesota, MN)]; hexanoic acid, octanoic acid [Acros Organics (NJ)]; decanoic acid, heptadecafluorononanoic acid, heptafluorobutyric acid, heptanoic acid, lauric acid, myristic acid, nonadecafluorodecanoic acid, pentadecafluorooctanoic acid, perfluorododecanoic acid, pentafluoropropionic acid, tridecafluoroheptanoic acid, tridecanoic acid, undecanoic acid, valeric acid [Aldrich Chemical Co. (Milwaukee, WI)]; butyric acid, trifluoroacetic acid [Caledon Laboratories Ltd. (Georgetown, ON)]; acetic acid, propionic acid [Fisher Scientific Co. (Fair Lawn, NJ)]; nonafluoropentanoic acid [Fluka (Oakville, ON)]; perfluorohexanoic acid [Oakwood Products Inc. (West Columbia, SC)]; nonanoic acid [Sigma Chemical Co. (St. Louis, MO)]; dimethyl- $d_6$  sulfoxide, DMSO- $d_6$  (D 99.9%) [Cambridge Isotope Laboratories, Inc. (Andover, MA)]. All chemicals and solvents were of 95% purity or greater and were used without alteration.

**2.1. NMR Spectrometer Parameters.**  $^1\text{H}$  NMR spectra were obtained with use of a Nalorac 5-mm  $^1\text{H}$  observe probe and a Varian 5-mm  $^1\text{H}$  indirect  $z$ -gradients equipped probe each tuned to 500 MHz for  $^1\text{H}$  resonance. All chemical shifts were recorded relative to tetramethylsilane (TMS, 0.000 ppm). The  $90^\circ$  pulse widths were  $12.25 \mu\text{s}$  for the Nalorac probe and  $5.2 \mu\text{s}$  for the Varian probe. The one-dimensional  $^1\text{H}$  NMR spectra were obtained by using a spectral width of 7998.4 Hz, acquisition time of 2.048 s, and one transient.  $^1\text{H}$   $T_1$  were determined by using an inversion recovery pulse sequence, spectral width of 7998.4 Hz, acquisition time of 2.048 s, one transient, recycle delay of 20 s, and 16381 points. Line broadening of 0.2 Hz and an exponential fit were applied for analysis. Spin–spin relaxation times ( $T_2$ ) were determined by using the Carr–Purcell Meiboom–Gill (CPMG) spin–echo pulse sequence with a spectral width of 1849.1 Hz, acquisition time of 2.049 s, four transients, recycle delay of 30 s, and 3788 points. “Big tau” was arrayed as follows: 0.064, 0.128, 0.256, 0.512, 1.024, 2.048, and 4.096 s. Line broadening of 0.6 Hz and an exponential fit were applied for analysis.

$^{19}\text{F}$  NMR spectra were obtained with a Nalorac 5-mm  $^{19}\text{F}$  observe probe tuned to 470 MHz for  $^{19}\text{F}$  resonance. The chemical shifts were recorded relative to  $\text{CFCl}_3$  (0.000 ppm). The  $90^\circ$  pulse width was  $6.75 \mu\text{s}$  for all  $^{19}\text{F}$  experiments. 1D  $^{19}\text{F}$  NMR spectra were obtained with a spectral width of 30581.0 Hz, acquisition time of 0.64 s, one transient, and a recycle delay of 10 s. 1D  $^{19}\text{F}$  variable-temperature experiments were conducted by using the identical parameters as above and increasing the temperature from 30 to 100 °C in 10 deg increments.  $T_1$  times were determined with an inversion recovery pulse sequence, spectral width of 52631.6 Hz, acquisition time of 0.64 s, one transient, recycle delay of 9.600 s, and 33684 points. Line broadening of 11.2 Hz and an exponential fit was applied for analysis.  $T_2$  times were determined by using the Carr–Purcell Meiboom–Gill (CPMG) spin–echo pulse sequence with a spectral width of 52631.6 Hz, acquisition time of 0.640 s, four transients, recycle delay of 30.000 s, and 33694 points. The “big tau” arrays were adjusted for the spin–lattice relaxation times. Line broadening of 11.20 Hz and an exponential fit were applied for analysis.

2D  $^{19}\text{F}$  NMR spectra were obtained by using a  $J$ -resolved pulse sequence with a spectral width of 30581.0 Hz in the direct

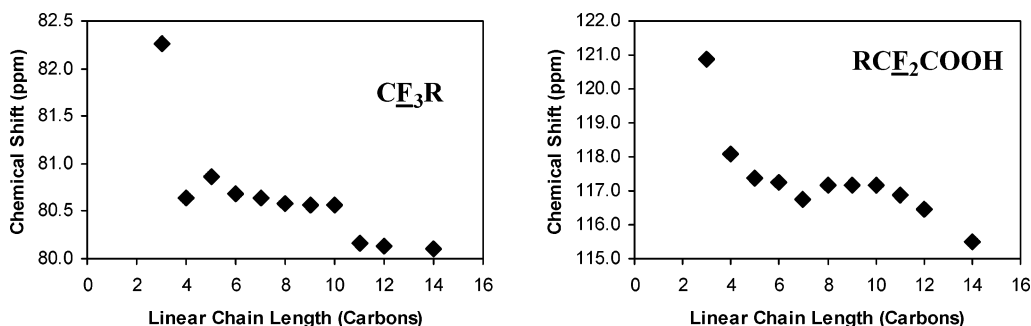


**Figure 1.**  $^{19}\text{F}$  NMR chemical shift change for the  $\text{CF}_3\text{R}$  and  $\text{RCF}_2\text{COOH}$  nuclei as a function of chain length.

dimension (F2), spectral width of 50.0 Hz in the indirect dimension (F1), acquisition time of 0.134 s, and a recycle delay of 6.3 s. The number of transients and increments varied according to the sample. The data were forward linear predicted to 512 points in the indirect dimension and apodized with a mixture of sine-bell and Gaussian weightings along both dimensions. The data were zero-filled to 8192 points in the direct dimension and 1024 complex points in the indirect dimension.

### 3. Results and Discussion

**3.1. Using  $^{19}\text{F}$  NMR To Ascertain Changes in the Geometry of PFCAs in DMSO- $d_6$  as a Function of Their Carbon Chain Length: A Link to Their Behavior in the Aquatic Environment.** NMR results given in the following sections refer to experiments conducted in DMSO- $d_6$ , used as a surrogate for water. It was necessary to use DMSO in place of water due to the enhancement in spectral resolution and also due to the requirement of a higher boiling solvent to conduct variable-temperature NMR experiments. Although DMSO is an aprotic solvent it serves as a reasonable surrogate for water due to its polarity. It is reasonable to assume that conformational results obtained with DMSO will have no significant difference in comparison to those which would be observed in water, as was observed in the case of conformational studies of Scylliorhinin I.<sup>27</sup> Therefore, it is reasonable to extend the results obtained for the DMSO systems to the aquatic environment.

**3.1.1. Chemical Shift ( $\delta$ ) Changes as a Function of Carbon Chain Length and Fluorination.** The chemical shift of the fluorine nucleus is a function of the shielding constants that describe the electron density around the nucleus. The observed shielding constant is a sum of several individual constants, most of which are identical for all of the analytes investigated here, and thus will not be discussed further in the current context. The shielding constant that has the largest impact upon chemical shift is the constant that is governed by van der Waals interactions with the surrounding solvent molecules. Thus, when a significant change in the chemical shift of a specific fluorine nucleus is observed due to the alteration of the molecule in a position that has no direct influence on the electron density at the said nucleus, it can be concluded that the alterations made to the molecule must have changed the interaction of the molecule with the solvent cage. This in turn leads to the conclusion the molecule has undergone a geometrical structure alteration.

The change in  $^{19}\text{F}$  NMR chemical shift,  $\delta$ , for the terminal  $\text{CF}_3$  and the  $\text{CF}_2$  adjacent to the carboxylic acid functionality, as a function of the length of the fluorinated chain, is depicted in the graphs shown in Figure 1. In the case of the C3 acid, it can be seen that the chemical shifts of both moieties are significantly different from those of the other longer chain acids, due to the lack of separation of the  $\text{CF}_3$  and  $\text{CF}_2$  from the  $\text{COOH}$ . In the case of the C5–C10 acids there is little change

in the chemical shift of the  $\text{CF}_3$ , suggesting that it remains in much the same electronic environment within each of these acids. As the fluorocarbon chain length is increased beyond C10, C11–C14, it can be seen that there is a noticeable decrease in the chemical shift associated with the  $\text{CF}_3$ . The chemical shift remains essentially constant for the C11–C14 acids (RSD < 0.01 ppm). Thus, the electronic environment of the  $\text{CF}_3$  undergoes an important alteration at >C10. This is in good agreement with other researchers' observations that the solid-state structure of the molecule adopts a partial helical conformation when the fluorocarbon chain is between 8 and 12 carbons in length.<sup>15–17</sup>

The observations based upon the  $\text{CF}_3$  are supported by similar trends observed for the  $\text{CF}_2$  adjacent to the function group. This leads to the conclusion that the molecule, as a whole, adopts a significant new conformation at an acid chain length of >C10 carbons.

**3.1.2. The Measurement of Spin–Lattice Relaxation as a Function of Carbon Chain Length and Fluorination: A Comparison with Hydrogen.** The change in spin–lattice ( $T_1$ ) relaxation as a function of increasing the perfluorinated acid chain length is shown in Figure 2a.  $T_1$  measurements were taken for three different fluorinated groups within the carbon chain; the  $\text{CF}_3$ , the  $\text{CF}_2$  adjacent to the  $\text{CF}_3$ , and the  $\text{CF}_2$  adjacent to the carboxylic acid functional group. Recording  $T_1$  values for each of these groups allowed an overall picture of the entire fluorinated chain to be developed. Each of the groups essentially behaved in the same way, with the same general trends being observed. Relaxation times were observably longer for the  $\text{CF}_3$  moiety when compared with the two internal  $\text{CF}_2$  groups. It can be seen from the graph that for each of the “CF” groups, there is a linear decrease in the time of relaxation as the acid chain length is increased from C2 to C9. This indicates that there is no significant change in the relative geometry of the chain as the chain length is increased from C2 to C9, as the rate of change for each of the groups is approximately the same. It is therefore hypothesized that the changes in relaxation associated with an increase in chain length are a direct result of the molecular size increase altering the dimensions and geometry of the solvent cage associated with the solute. This hypothesis is supported by theory, which states that for spin- $1/2$  nuclei, such as  $^{19}\text{F}$ , relaxation phenomena are dominated by dipolar interactions between nuclei, modulated by molecular motions.<sup>28</sup> It is known<sup>28</sup> that these relaxation rates depend on the following parameters: temperature, solution viscosity, molecular size and structure, and in some circumstances the applied magnetic field. In the systems investigated in these studies the parameters temperature, solution viscosity, and the applied magnetic field remained constant. Thus, the observed changes in  $T_1$  are assumed to be a direct result of molecular size and structure alterations. As the molecular size increased

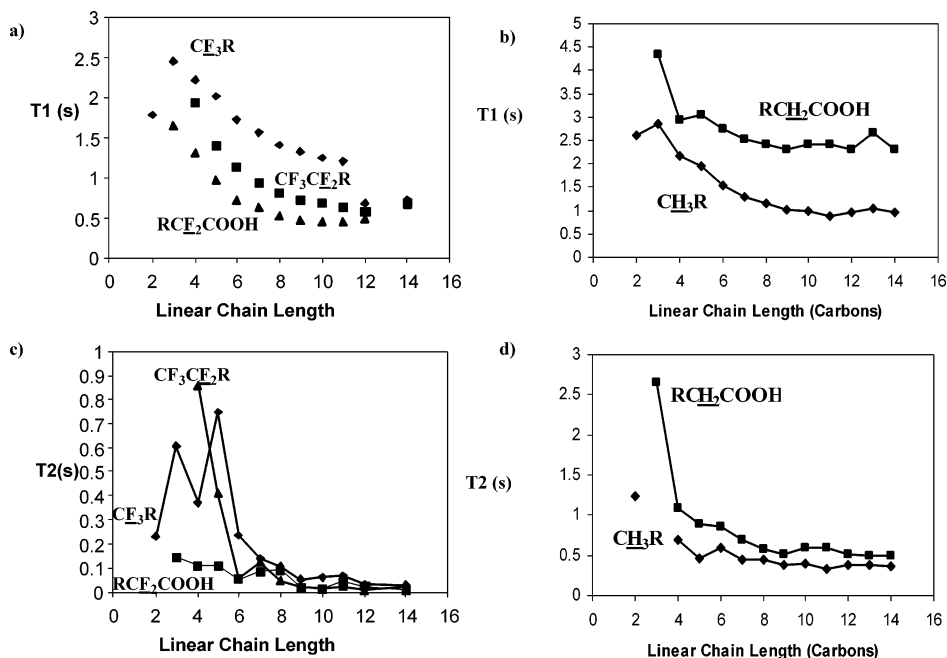


**Figure 2.** Comparisons of relaxation times for fluorine nuclei and protons as a function of carbon chain length. (a)  $T_1$  relaxation for the  $\text{CF}_3\text{R}$ ,  $\text{CF}_3\text{CF}_2\text{R}$ , and  $\text{RCF}_2\text{COOH}$  nuclei. (b)  $T_1$  relaxation for the  $\text{CH}_3\text{R}$  and  $\text{RCH}_2\text{COOH}$  nuclei. (c)  $T_2$  relaxation for the  $\text{CF}_3\text{R}$ ,  $\text{CF}_3\text{CF}_2\text{R}$ , and  $\text{RCF}_2\text{COOH}$  nuclei. (d)  $T_2$  relaxation for the  $\text{CH}_3\text{R}$  and  $\text{RCH}_2\text{COOH}$  nuclei.

linearly as the carbon chain was increased, deviations from a linear change in the  $T_1$  times can logically be attributed to a structural alteration. Therefore, for the acids C2–C9, changes in  $T_1$  times appear to only occur due to size increase with no significant structural deviations occurring.

As was seen in the chemical shift changes associated with increasing the carbon chain length, there appears to be a distinct change in the relaxation of the molecule as the chain length is increased beyond C10, and by C14 the relaxation is equivalent for all three groups investigated. The most significant change in  $T_1$  times is observed for the  $\text{CF}_3$  group. This trend can again be attributed to a distinct change in the molecular geometry of the molecule at these chain lengths, and hence a change in the solvation of the molecule, which in turn leads to changes in the mechanism of relaxation. As each of the CF groups no longer behave similarly, it is reasonable to assume that in this new adopted geometry the solvation of the segment of the molecule is significantly different.

A direct comparison of these  $T_1$  findings for perfluorinated acids was made with their hydrogenated counterparts, Figure 2b. From the figure it can be seen that the same trends are observed for the  $\text{CH}_3$  as were seen for the  $\text{CF}_3$  as the chain length is increased, namely a linear reduction in  $T_1$  as a function of size. This supports the hypothesis that relaxation is simply a function of the geometry and distribution of the solvent cage, rather than being specific to fluorination. No dramatic change in the  $T_1$  times is observed when the chain length increases from C11 to C14 for either the  $\text{CH}_3$  or the  $\text{CH}_2$  attached to the carboxylate functional group. This lends credence to the idea that the changes observed for the fluorinated acids are due to a change in molecular geometry entirely associated with the incorporation of fluorine within the molecule.

Thus, the incorporation of fluorine within the carboxylic acid leads to structural changes within the molecule that are not observed for their hydrogenated counterparts. Furthermore, these effects are highly dependent upon the size of the fluorocarbon chain length. The effect that fluorine imparts upon the molecule cannot be viewed simply as the sum of the number of fluorine atoms contained within the molecule.

**3.1.3. The Measurement of Spin–Spin Relaxation as a Function of Carbon Chain Length and Fluorination.** The  $T_2$  relaxation times were measured for the perfluorinated acids as a function of their chain length (Figure 2c). Results are presented for the  $\text{CF}_3$ , the  $\text{CF}_2$  adjacent to the  $\text{CF}_3$ , and the  $\text{CF}_2$  adjacent to the carboxylic acid functional group. It can be seen that the relaxation for each of the CF groups is significantly different. The relaxation of the  $\text{CF}_3$  moiety for the acids C2–C6 varies considerably, and no discernible trend is observed. For the acids C6–C10, there is a linear decrease in  $T_2$ , suggesting that for these acids the relaxation is simply a function of chain length. For the acids >C10, there is little change in the relaxation. As was seen with the previously measured parameters, chemical shift and  $T_1$ , these results suggest that there is no significant change in molecular geometry as the fluorocarbon chain length is increased from 7 carbon atoms to approximately 10. The other two CF units for which  $T_2$  was measured do not show as much variability in their values when compared with the  $\text{CF}_3$ . The trends for these two groups are less evident than for the  $\text{CF}_3$ ; however, the small trends observed also support the hypothesis that there is a conformational change in the fluorocarbon chain at approximately 10 carbon units.

When comparing and contrasting the  $T_2$  times measured for the hydrogenated analogues of the perfluorinated acids, Figure 2d, it can be seen that there is little change in the relaxation of the  $\text{CH}_3$  and the  $\text{CH}_2$  adjacent to the carboxylic acid functional group for the acids C5–C14. Again, this supports the idea that the geometry of the fluorinated acids is strongly influenced by the incorporation of fluorine, which is not seen for hydrocarbon acids.

**3.1.4. Application of an  $^{19}\text{F}$  2D J-Resolved Pulse Sequence for Establishing Coupling Constants and Molecular Geometry.** The measurement of scalar coupling constants for perfluorinated acids is difficult due to long-range  $^{19}\text{F}$ – $^{19}\text{F}$  coupling and spectral overlap.<sup>19,20</sup> For even the relatively small perfluorinated acids, such as heptafluorobutyric acid, the coupling constants associated with it have been largely indiscernible.<sup>20</sup> To the best of our knowledge, no research has been reported concerning the

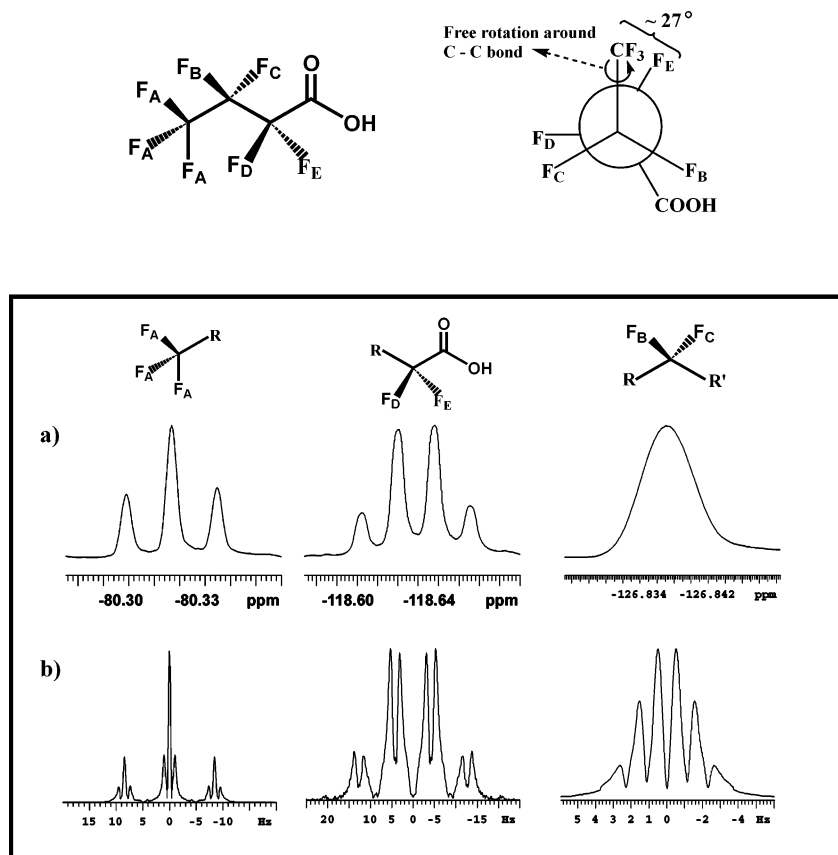


**Figure 3.** (a) 1D  $^{19}\text{F}$  NMR for heptafluorobutyric acid and (b) 2D  $J$ -resolved NMR of the same molecule. A Newman projection of the acid conformation is indicated.

measurement of the molecular conformation of these small-chain perfluorinated acids in solution.

A typical 1D  $^{19}\text{F}$  NMR for heptafluorobutyric acid is shown in Figure 3a. As can be seen from this spectrum, and as is reported in the literature,<sup>20</sup> the large  $^4J_{\text{FA}-\text{FD}}$  coupling constant of 8.45 Hz is the only discernible coupling constant.

The ability to measure the coupling constants of all the fluorine nuclei within these acids in solution would facilitate the interpretation of the molecular geometries and conformation of these molecules. This is especially true in the case of the conformations of acids that are in the liquid state at room temperature, and thus are not amenable to X-ray crystallography techniques.

We have therefore applied a 2D  $J$ -resolved pulse sequence for the acids. Figure 3b shows how the 1D NMR spectrum becomes conveniently separated and well resolved based upon the coupling constants of the individual fluorine nuclei. Interpretation of the coupling for heptafluorobutyric acid gives  $^4J_{\text{FA}-\text{FD}} = 8.45$  Hz,  $^3J_{\text{FA}-\text{FBFC}} = 1.10$  Hz,  $^3J_{\text{FB}-\text{FD}}/{}^3J_{\text{FC}-\text{DFE}} = 2.19$  and 1.10 Hz, and  $^1J_{\text{FBFC}}$  and  $^1J_{\text{DFE}} < 0.01$  Hz. A Varian NMR modeling simulation using these interpreted coupling constants resulted in a spectrum that was indistinguishable.

The splitting pattern observed for the heptafluorobutyric acid indicated that the fluorine atoms within each of the  $\text{CF}_2$  moieties are nonequivalent, and that all three fluorine atoms on the  $\text{CF}_3$  group are equivalent, resulting in a  $\text{A3MNXY}$  spin system. For this to be the case, the fluorocarbon chain must be held reasonably rigid while there is free rotation of the  $\text{CF}_3$  group. The energetically favored conformation of the fluorinated chain in solution cannot be zigzag in nature, although this was the solid state structure previously suggested,<sup>15</sup> and must adopt a conformation similar to that shown in the Newman projection (Figure 3).

**TABLE 1: Selected  $\text{CF}_3$  and  $\text{CF}_3\text{CF}_2\text{CF}_2$   $^{19}\text{F}$ – $^{19}\text{F}$  Coupling Constants as a Function of Fluorocarbon Chain Length**

acid	$^3J_{\text{F1}-\text{F3}}$ (Hz)
heptafluorobutyric acid	8.45
nonafluoropentanoic acid	9.64
perfluorohexanoic acid	9.80
tridecafluoroheptanoic acid	9.80
pentadecafluorooctanoic acid	9.80
heptadecafluorononanoic acid	10.15
nonadecafluorodecanoic acid	10.15

This pulse sequence was applied to longer chain acids and proved to be invaluable in ascertaining their coupling constants. Although the majority of these coupling constants still need to be fully established and are not presented herein, an important observation has been made concerning the coupling between the  $\text{CF}_3$  and the  $\text{CF}_2$  group located one carbon removed from the  $\text{CF}_3$ . The coupling constants between these two groups are presented in Table 1 as a function of chain length. As can be seen from the table, the magnitude of the coupling constant remains effectively the same for the acids C6–C8, with change in the constant observed for >C9. It is accepted that an alteration in the dihedral bond angles of a molecule will result in a change in the magnitude of the coupling constants.<sup>29</sup> Thus, these results are in accordance with the change in conformation of the molecule as the fluorocarbon chain increases beyond approximately 9–10 carbon atoms. Unfortunately, the prediction of  $^{19}\text{F}$ – $^{19}\text{F}$  coupling constants with respect to dihedral angle, and vice versa, remains difficult due to significant Ramsey term contributions which do not appear to sustain a classic Karplus dependence.<sup>29</sup> Thus, from the standpoint of this research it can only be concluded that empirically the magnitude of the coupling changes thus too must the geometry and bond angles of the molecule.

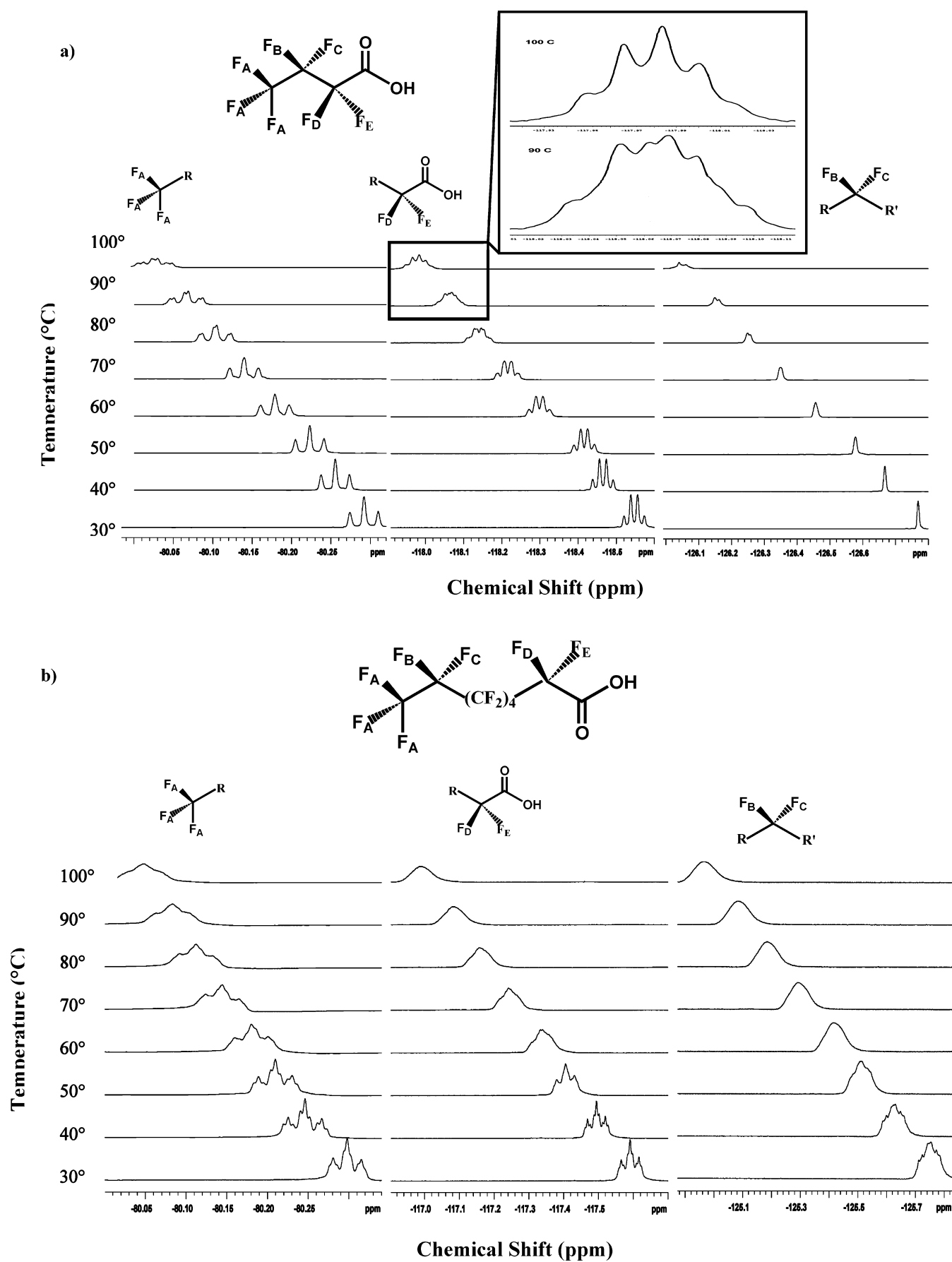


**Figure 4.** Comparison of variable-temperature  $^{19}\text{F}$  NMR of (a) heptafluorobutyric acid and (b) pentadecafluorooctanoic acid. Spectra recorded between 40 and 100  $^\circ\text{C}$  are offset from 30  $^\circ\text{C}$  spectrum for illustrative purposes. The relative chemical shifts remain the same throughout, small changes can be attributed to changes in the solvent due to temperature.

PFCAs would therefore appear to adopt a helical twist conformation in solution phase, even in the case of small carbon chain lengths. Taken in connection with the results which were observed for the dependence of chemical shift and relaxation it would appear that observed changes in geometry at C10 must be due to a change in the dihedral angle of the molecule, indicating that the helical twist changes in magnitude as the chain length increases. The exact magnitude of this angle change is not known, and it is difficult to predict as there is likely no simple Karplus relationship for these compounds.<sup>29</sup>

**3.1.5. The Use of Variable-Temperature <sup>19</sup>F 1D NMR in Establishing Molecular Rigidity.** A variable-temperature 1D <sup>19</sup>F NMR experiment was conducted for heptafluorobutyric and pentadecafluorooctanoic acid. NMR spectra were collected over a 30–100 °C range, in increments of 10 deg. An NMR stack plot for each of the acids is shown in Figure 4. As can be seen from Figure 4a, a lack of coherence, i.e., a broadening of the spectrum, is observed in the splitting pattern for the butyric acid at approximately 40 °C. For example, the line width of the signal for the CF<sub>2</sub>FC group doubles at this point. At this temperature, the previously inflexible backbone of the perfluorocarbon chain starts to become flexible, causing a broadening of the spectrum. The NMR spectrum becomes well resolved once more at a temperature of 90 °C, at which point all the molecules present are energetically able to undergo free rotation. It would appear from the spectra obtained at 100 °C that two predominant conformations exist. These are likely to be the unequal populations of the helical and zigzag conformers. Further investigations of the nature of the conformers at elevated temperatures are required.

In comparison, the NMR temperature-dependent spectra obtained for the perfluorooctanoic acid, shown in Figure 4b, indicated that free rotation within the fluorocarbon chain again starts to occur at approximately 60 °C. However, the spectra do not become resolved at temperatures below 100 °C, indicating that, energetically, the chain is more rigid than was the case for the heptafluorobutyric acid. These results are in keeping with those that have been previously reported in the literature for other C8 fluorocarbon chains.<sup>14</sup> Thus, it can be concluded that, in the case of fluoro-surfactant carboxylic acids in solution, chain rigidity increases as a function of the fluorocarbon chain length. It is recognized that an alternate explanation for the change in spectral properties at elevated temperatures could be the complexation of the carboxylic acids with the DMSO. To completely eliminate this possibility further investigations are required with solvents that do not allow such interactions.

It can be concluded that any environmental process that requires, or is influenced by, molecular rigidity will therefore be influenced as a function of the perfluoro chain length of the PFCA. The stability of the molecule or the energy required to fold the molecule will be affected. One such physical property would be the vapor pressure of the PFCAs. One would predict, on the basis of these results, that the rate of decrease in vapor pressure as a function of the chain length would not follow a linear or conventionally anticipated trend.

#### 4. Connection of <sup>19</sup>F NMR Results with the Empirically Observed Physical Properties

The hypothesized changes in geometric structure of the fluorinated chain are reflected in the observed physical properties. For example, the variations in melting point of the acids, with increase in the chain length, are consistent with the idea of a change in geometry that starts to occur at approximately C8 (Figure 5a). The effect is also seen in the boiling point of

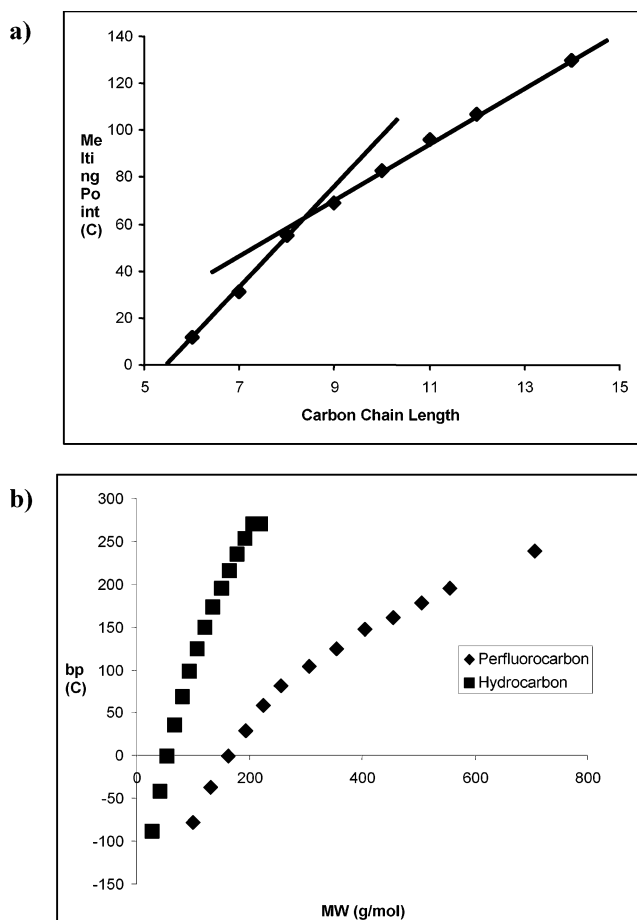


**Figure 5.** (a) The melting point of perfluorocarboxylic acids as a function of carbon chain length, (b) The boiling point of perfluoroalkanes as a function of carbon chain length expressed as molecular weight compared with their hydrocarbon counterparts. Data were taken from ref 30.

fluorinated alkanes and is not observed in their hydrocarbon counterparts (Figure 5b).

**Acknowledgment.** This work was partially supported by a Strategic Project Grant from the National Sciences and Research Council of Canada (NSERC). The authors also wish to thank the Pennsylvania State University Schreyer Honors College for providing an International Thesis Research Grant that allowed collaboration between The University of Toronto and Pennsylvania State University, without which this research could not have been conducted.

#### References and Notes

- (1) Holloway, J. H. *J. Fluorine Chem.* **2000**, *104*, 3.
- (2) Kissa, E. *Fluorinated Surfactants, Synthesis, Properties, Applications*; Marcel Dekker: New York, 1994.
- (3) Kannan, K.; Newsted, J.; Halbrook, R. S.; Giesy, J. P. *Environ. Sci. Technol.* **2002**, *36*, 2566.
- (4) Hansen, K. J.; Johnson, H. O.; Eldridge, J. S.; Butenhoff, J. L.; Dick, L. A. *Environ. Sci. Technol.* **2002**, *36*, 1681.
- (5) Kannan, K.; Hansen, K. J.; Wade, T. L.; Giesy, J. P. *Arch. Environ. Contam. Toxicol.* **2002**, *42*, 313.
- (6) Kannan, K.; Franson, J. C.; Bowerman, W. W.; Hansen, K. J.; Jones, J. D.; Giesy, J. P. *Environ. Sci. Technol.* **2001**, *35*, 3065.
- (7) Giesy, J. P.; Kannan, K. *Environ. Sci. Technol.* **2001**, *35*, 1339.
- (8) Moody, C. A.; Kwan, W. C.; Martin, J. W.; Muir, D. C. G.; Mabury, S. A. *Anal. Chem.* **2001**, *73*, 2200.
- (9) Moody, C. A.; Martin, J. W.; Kwan, W. C.; Muir, D. C. G.; Mabury, S. A. *Environ. Sci. Technol.* **2002**, *36*, 545.
- (10) Ellis, D. A.; Mabury, S. A.; Martin, J. W.; Muir, D. C. G. *Nature* **2001**, *412*, 321.

- (11) US EPA. World Wide Web site: <http://www.epa.gov/opptintr/pfoa/index.htm>.
- (12) Ellis, D. A.; Mabury, S. A. *J. Am. Soc. Mass Spectrom.* **2003**, *14*, 1177.
- (13) Stock, N. L.; Ellis, D. A.; Deleebeeck, L.; Muir, D. C. G.; Mabury, S. A. *Environ. Sci. Technol.* **2004**, *38*, 1693.
- (14) Eaton, D. F.; Smart, B. E. *J. Am. Chem. Soc.* **1990**, *112*, 2821.
- (15) Wang, J. G.; Ober, C. K. *Liq. Cryst.* **1999**, *26*, 637.
- (16) Knochenhauer, G.; Reiche, J.; Brehmer, L.; Barberka, T.; Woolley, M.; Tredgold, R.; Hodge, P. *J. Chem. Soc., Chem. Commun.* **1995**, 1619.
- (17) Erkoç, S.; Erkoç, F. *J. Mol. Struct. (THEOCHEM)* **2001**, *549*, 289.
- (18) Dvinskikh, S. V.; Furu, I. *Langmuir* **2000**, *16*, 2962.
- (19) Yonemori, S.; Sasakura, H. *J. Fluorine Chem.* **1995**, *75*, 151.
- (20) Emsley, J. W.; Feeney, J.; Sutcliffe, L. J. *High-Resolution Magnetic Resonance Spectroscopy*; Pergamon: New York, 1966; Vol. 2, p 877.
- (21) Weigert, P. J.; Karel, K. J. *J. Fluorine Chem.* **1987**, *37*, 125.
- (22) Bauduin, G.; Boutevin, B.; Pietrasanta, Y. *J. Fluorine Chem.* **1995**, *71*, 39.
- (23) Ribeiro, A. A. *Magn. Reson. Chem.* **1997**, *35*, 215.
- (24) Serratrice, G.; Stebe, M. J.; Delpuech, J. J. *J. Fluorine Chem.* **1984**, *25*, 275.
- (25) Von Werner, K.; Wrackmeyer, B. *J. Fluorine Chem.* **1981**, *19*, 163.
- (26) Von Werner, K.; Wrackmeyer, B. *J. Fluorine Chem.* **1986**, *31*, 183.
- (27) Rodziewicz-Motowidlo, S.; Legowska, A.; Qi, X.-F.; Czaplowski, C.; Liwo, A.; Sowinski, P.; Mozga, W.; Olczak, J.; Zabrocki, J.; Rolka, K. *J. Peptide Res.* **2000**, *56*, 132.
- (28) Derome, A. E. In *Modern NMR Techniques for Chemistry*; Baldwin, J. E., P. Magnus, D., Eds.; Pergamon: New York, 1987; Vol. 6.
- (29) Kurtkaya, S.; Barone, V.; Peralta, J. E.; Contreras, R. H.; Snyder, J. P. *J. Am. Chem. Soc.* **2002**, *124*, 9702.
- (30) Ellis, D. A.; Cahill, T. M.; Mabury, S. A.; Cousins, I.; MacKay, D. Partitioning of Organofluorine Compounds in the Environment. In *The Handbook of Environmental Chemistry*; Neilson, A., Ed.; Springer: Berlin, Germany, 2002; Vol. 3, Part N, pp 63–83.